Improved Analysis of Propagation over Irregular Terrain

Vladimír SCHEJBAL

Jan Perner Faculty of Transport, University of Pardubice, Studentská 95, 532 10 Pardubice, Czech Republic

vladimir.schejbal@upce.cz

Abstract. *An improved analysis of propagation over irregular terrain using physical optics approximation of vector problem is presented. It offers more reliable numerical simulations for low altitude propagation and diffraction field zone without any auxiliary procedures. Numerical simulations are compared with measurement results and various approximate methods.*

Keywords

Electromagnetic propagation, electromagnetic propagation terrain factors, low altitudes propagation, numerical simulation.

1. Introduction

Propagation of electromagnetic waves over terrain is very challenging for various problems such as communications, radar coverage and antenna far-field measuring range. The geometrical optics and various GTD modifications could be used [1] but GTD fails to predict fields at caustics. An integral equation approach [2] is very slow and neglect backscattering, which plays an important role in field calculations, particularly in deep shadow regions. The algorithms [3] provide considerable savings in processing time for the solution of an integral equation. Irregular terrain reflection computations can be found in [4]. Due to the small storage capacity of the Elliott 503 computer, it was necessary to simplify the vector solution to a great extent, and therefore the scalar solutions were only considered for computation. The same result could be derived using Franz formula [5]. That was used for vector solutions. The comparison of numerical simulations and computation accuracy were presented in [6], [7] and [8] for propagation over irregular terrain and the finite distance between the antenna and the observation point (diffraction field zone) for higher and low altitude propagation, when knife-edge diffraction and Fock's spherical surface solution were used. Numerical simulations, measurements and published solutions for individual special cases agree quite well. Thanks to very efficient numerical integration it was possible to solve various problems such as radar coverage diagrams, radar site analysis and antenna far-field measurement ranges [9].

This paper describes a new improved analysis of electromagnetic wave propagation over irregular terrain using physical optics approximation of vector problem. Numerical simulations are compared with measurement results and various approximate methods. That allows more reliable computations for low altitude propagations and diffraction field zone.

2. Propagation over Irregular Terrain

Let us consider the antenna *A* over the earth surface as shown in Fig. 1. The total field everywhere could be calculated as the sum of the incident wave and the scattered field. The resultant electric vector $\boldsymbol{E}$(P) at the point P is given by

$$\boldsymbol{E}(\mathrm{P}) = \boldsymbol{E}_i(\mathrm{P}) + \boldsymbol{E}_s(\mathrm{P}) \tag{1}$$

where $\boldsymbol{E}_i$(P) is the incident electric vector, and $\boldsymbol{E}_s$(P) is the scattered electric vector. The incident field could be considered as a spherical wave at any reflecting point. It could be decomposed into two parts (parallel and perpendicular to the incident plane). According to the equivalence principle, a real scattering object is replaced by the equivalent currents induced on its surface, i.e. a distribution of equivalent sources in free space should be considered, which radiate without restraint in all directions. If these sources were determined correctly that would provide the correct solution to the scattering problem.

Scattering of electromagnetic waves by arbitrary opaque objects with local reflection coefficient can be determined using physical optics (PO) approximation ([10], Sect. 4.2 Vector Problem). The terrain surface could be divided into S_{il} and S_{sh} (illuminated and shadowed parts) with a shadow contour between them, as is shown in Fig. 1. According to PO approximation, the field induced on the surface of the object is determined by geometrical optics. That defines the induced sources only on the illuminated part, S_{il}, of the scattering object. On the shadowed part, S_{sh}, these components are set to zero.

Using principle of stationary phase [11]

$$\int_{-\infty}^{\infty} \exp\left(-j\pi z^2/2\right) dz = \sqrt{2}\exp\left(-j\pi/4\right), \tag{2}$$

the propagation over a terrain (the PO approximation of the vector problem with 3-D surface) can be approximated by the propagation over a 2-D surface. According to [4] – [6]

the following equation can be derived for the horizontal polarization component $E_{sz}(\mathrm{P})$ and the maximum value of incident electric vector E_0 at a distance R_0

$$\frac{E_{sz}(\mathrm{P})}{|E_0|}=\frac{R_0 e^{j\pi/4}}{2\sqrt{\lambda}}\int_a^b f(\theta_1)[(1-\Gamma)\sin(\theta_1-\alpha)+(1+\Gamma)$$

$$\times\sin(\theta_2-\alpha)]\frac{e^{-jk(R_1+R_2-R_0)}}{\sqrt{R_1R_2(R_1+R_2)}}\frac{dx}{\cos\alpha} \qquad (3)$$

where R_0, R_1, R_2, θ_1, θ_2 and α are shown in Fig. 1, $f(\theta_1)$ is the normalized antenna radiation pattern with phase center at point A at height h_A over the terrain, Γ is the Fresnel reflection coefficient (local reflection coefficient), $k = 2\pi/\lambda$, λ is the wavelength and a, b are limits of the illuminated part S_{il}. A rather analogous approach is used in [2]. A similar equation can be derived for vertical polarization using H_{sz} [5]. Therefore, this method takes into account the polarization.

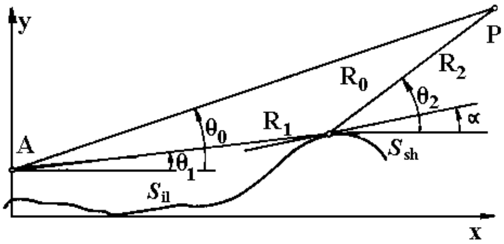

Fig. 1. Propagation geometry.

The reflection coefficient for a surface with random deviations could be approximated by

$$\Gamma = \Gamma_0 \exp\left[-2(2\pi\sigma\sin\gamma_0/\lambda)^2\right] \qquad (4)$$

where σ is the surface standard deviation, Γ_0 is the local Fresnel reflection coefficient for the smooth surface for the horizontal (or vertical) polarization, and γ_0 is the grazing (reflection) angle - the angle between the tangent and the incident (reflected) ray.

Numerical simulations, measurements and published solutions have validated individual special cases [4] – [8] of the described method (3). That has been extensively used for higher altitude propagation computations of radar coverage, radar site studies (comparison of numerical computations and flight test are given in [5], [9]) and analyses of various antenna far-field measurement ranges.

The terrain profile of the antenna far-field measurement range is shown in Fig. 2. One example of measured and calculated values of $A = 20\log|E(\mathrm{P})/E_0|$, where $\boldsymbol{E}(\mathrm{P})$ is the resultant electric vector, is shown in Fig. 3 for antenna far-field measurement range (the value of $h = 0$ corresponds to an origin of measurement scanner). The field was measured by a small horn to diminish a directivity effect of used horn with vertical scanning movement of 5 m. The transmitting antenna was on a tower with height of 10 m and a receiving antenna (horn) was placed on a tower with height of 16 m at the distance of 1 240 m. In this case, a shadowing object does not exist, and therefore the terrain between both antennas forms illuminated part. It can be seen that the measurement values are in agreement with the calculation. The differences could be explained by reflections from objects in the neighborhood of the horn such as a tower structure and guard rails and by reflection coefficient changes. That depends on terrain conditions (e.g. the earth surface could be covered by snow, plowed or overgrown by vegetation). It affects both reflected and total field but it is not usually substantial as the local reflection coefficient $\Gamma \approx -1$ for a low grazing angle regardless of polarization and surface standard deviation.

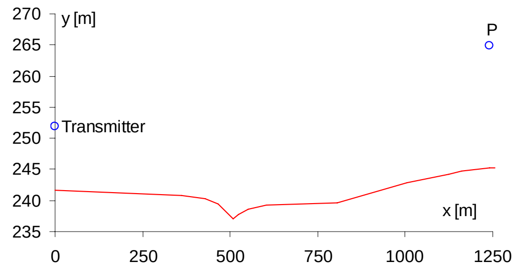

Fig. 2. Terrain profile of antenna far-field measurement range.

Several examples of calculations for antenna range (with terrain profile shown in Fig. 2) are shown in Fig. 4 for very dry surface ($\varepsilon_r = 3.2 - 0.015j$), very wet surface ($\varepsilon_r = 30 - 2.5j$) and surface with $\sigma = 0.2$ m and $\varepsilon_r = 3.2 - 0.015j$. It could be noted that the measurement was performed several times for various terrain conditions and changes due to various terrain conditions (summer, winter, snow or vegetation) were comparable with numerical simulations.

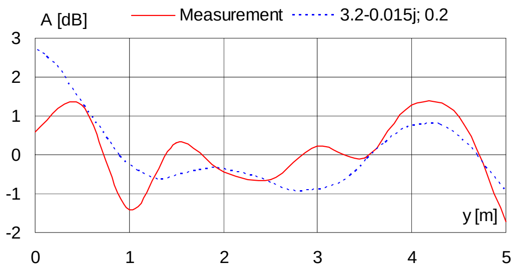

Fig. 3. Measured and calculated (for surface with $\sigma = 0.2$ m and $\varepsilon_r = 3.2 - 0.015j$) values of $A = 20\log|E(\mathrm{P})/E_0|$ for antenna far-field measurement range.

The previous computations of low altitude propagation (LAP) and transient zone (TZ) are described in detail [6]. The knife-edge diffraction [12] and Fock's spherical surface solution [13], which neglect terrain imperfections, were used for low altitude propagation. They are scalar solutions. These methods are well known and have been extensively used. They have been proven as very efficient approximate methods for real terrain both analytically and experimentally. The transient zone would be considered, if the differences between the reflected and incident rays were less than a third of the wavelength, and the low altitude would be considered, if the differences were less than $\lambda/2\pi$. Therefore the previous computations are relatively artificial as two quite different approximations are used for the computation and the transient zone limits are only supported by an ad hoc assumption.

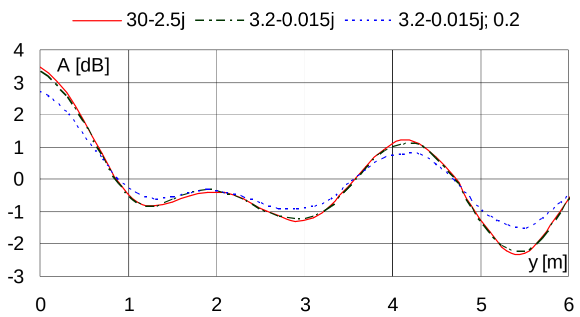

Fig. 4. Very dry surface (ε_r = 3.2 - 0.015j), very wet surface (ε_r = 30 - 2.5j), and surface with σ = 0.2 m and ε_r = 3.2 - 0.015j.

Considering Ufimtsev's results [10] a completely new approach to analyze propagation over irregular terrain could be used. The scattered field (3) can be divided into two parts, i.e. the reflected radiation component, E_{sz}^{ref}, (with the reflection coefficient Γ terms) and the shadow radiation component, E_{sz}^{sh}

$$S_{sz}^{ref}(P) = \frac{|E_0| R_0 e^{j\pi/4}}{2\sqrt{\lambda}} \int_a^b f(\theta_1)\Gamma[\sin(\theta_2-\alpha) - \sin(\theta_1-\alpha)] \times \frac{e^{-jk(R_1+R_2-R_0)}}{\sqrt{R_1 R_2 (R_1+R_2)}} \frac{dx}{\cos\alpha}, \tag{5}$$

$$S_{sz}^{sh}(P) = \frac{|E_0| R_0 e^{j\pi/4}}{2\sqrt{\lambda}} \int_a^b f(\theta_1)[\sin(\theta_2-\alpha) + \sin(\theta_1-\alpha)] \times \frac{e^{-jk(R_1+R_2-R_0)}}{\sqrt{R_1 R_2 (R_1+R_2)}} \frac{dx}{\cos\alpha}. \tag{6}$$

The reflected component, E_{sz}^{ref}, depends on the local reflection coefficient. On the other hand, the shadow radiation power is equal to the total power incident on a scattering object and it does not depend on the reflection coefficients. According to the shadow contour theorem, it does not depend on the whole shape of the scattering object and is completely determined only by the size and the geometry of the shadow contour. For the shadow region (such as shown in Fig. 5) at a finite distance from the scattering object (behind the object), the shadow radiation for very short wavelength can be considered as a wave beam that asymptotically cancels the incident field and the reflected beams asymptotically vanish. The shadow radiation gives origin to edge waves, creeping waves, and surface diffracted rays.

That means that equations (5) and (6) could be used for calculation for both illuminated and shadow region. The computation of scattered field (5) and (6) can be done for higher altitudes (greater differences between the reflected and incident rays) as well as for lower altitudes (i.e. it is not necessary to consider the low altitude propagation and transient zone). The numerical simulations using (5) and (6) offer much more consistent solution, which takes into account the polarization (even for the shadow region). Obviously, the calculations for higher altitudes (greater differences) are the same for the previous technique and the new method, when shadowing objects are not present. A similar approach can be used for vertical polarization.

Comparisons between the previous technique [6] and the new method have been done for various cases. The calculations for higher altitudes using the previous technique and the new method for propagation over a flat surface are the same and therefore are not shown. For the antenna far-field measurement range, the calculations shown in Fig. 3 are the same for the previous technique and the new method because shadowing objects are not present. Similarly, the previous and improved methods give the same results for the examples shown in Fig. 4.

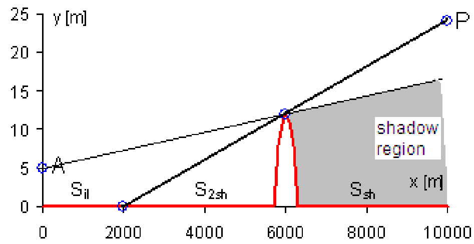

Fig. 5. Terrain considered for comparison of the previous and new methods.

The terrain shown in Fig. 5 is considered as one of various examples. The illuminated part of terrain, S_{il}, ranges from 0 to 6 000 m and the shadowed part ranges from 6 000 m to 10 000 m. The antenna coordinates are x_A = 0 m and $y_A = h_A$ = 5 m and point P coordinates x_P = 10 000 m and y_P are changing from 1 to 100 m. Reflection coefficients have been calculated for relative permittivity of 4 – 0.001j and σ = 0. The comparisons of the previous and improved methods are shown in Fig. 6.

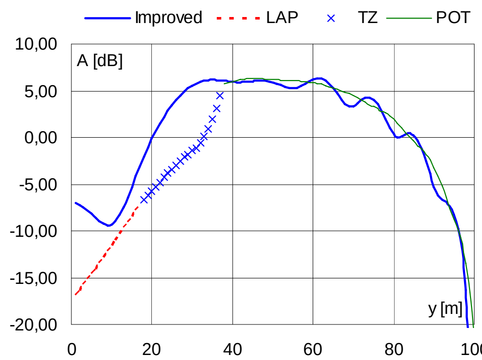

Fig. 6. Previous solution - low altitude propagation (LAP), transient zone (TZ) and calculation for higher altitudes (POT) and new method (Improved).

Naturally, the previous transient zone (TZ) and low altitude computations (LAP) using knife-edge diffraction approximations and Fock's spherical surface solutions, which neglect terrain imperfections, are only approximate solutions. The comparison of the previous solution for higher altitudes (POT) and the new (Improved) methods shows that only small differences exist. That is due to the fact that for the previous method, the second type of shadow, S_{2sh}, [6] is considered (see Fig. 5), where the integration is not performed (i.e. contributions are not considered because of the shadowing obstacle at $x = 6\,000$ m). On the other hand, the improved method actually replaces a real scattering object by the equivalent currents. Therefore the new approach to analyze propagation over irregular terrain could be much more accurate.

The problems of the described method are due to approximations accepted for the surface field. They could be diminished using the 2D physical theory of diffraction (PTD), which is a natural extension of physical optics. Similar approach is used in [14]. Moreover, paper [15] presents a new version of PTD without a grazing singularity. It is well suited for investigation of bistatic scattering, when both faces of the edge are illuminated. It introduces a new non-uniform component of the surface current. That generates elementary edge waves. The new version of PTD is valid for all scattering directions, including forward scattering.

3. Conclusions

Previous methods [4] – [8] have been frequently used for computations of higher altitudes as well as low altitude propagation. The knife-edge diffraction and Fock's spherical surface solution, which neglect terrain imperfections, were used for low altitude propagation in previous codes and they do not take into account the polarization. Various problems such as radar coverage diagrams and antenna far-field measurement ranges have been solved. Numerical simulations, measurements and published solutions have validated individual special cases. Therefore, the previous method could be used for comparison.

The paper describes the new improved analysis of electromagnetic wave propagation over irregular terrain considering reflected component and the shadow radiation component, which offers more reliable numerical simulations considering edge waves, creeping waves, and surface diffracted rays for low altitude propagation and diffraction field zone without any auxiliary approximate procedures. Therefore, the numerical simulations using (5) and (6) offer much more consistent solution, which takes into account the polarization.

The comparison of the previous and new methods shows that only small differences exist for higher altitudes. That is due to the fact that the second type of shadow, S_{2sh}, (shown in Fig. 5) for the previous method is considered. The previous transient zone and low altitude computations are only approximate. Therefore the improved analysis of propagation over irregular terrain could be much more useful and accurate.

The problems of the described method are due to approximations accepted for the surface field and could be diminished using the 2D physical theory of diffraction (PTD), which is a natural extension of physical optics. Moreover, the new version of PTD is valid for all scattering directions, including forward scattering.

Acknowledgements

The paper is supported by the Czech National Institutional Research "Theory of Transport System" No. MSM 0021627505. The author is thankful to the reviewers, whose suggestions helped a lot in improving the article.

References

[1] LUEBBERS, R. J. Propagation prediction for hilly terrain using GTD wedge diffraction. *IEEE Trans. Antennas Propag.*, 1984, vol. 32, no. 9, pp. 951 – 955.

[2] HVIID, J. T., ANDERSON, J. B., TOFTGÅRD, J. T., BØJER, J. Terrestrial-based propagation model for rural area — an integral equation approach. *IEEE Trans. Antennas Propag.,* 1995, vol. 43, no. 1, pp. 41–46.

[3] AKORLI, F. K., COSTA, E. An efficient solution of an integral equation applicable to simulation of propagation along irregular terrain. *IEEE Trans. Antennas Propag.,* 2001, vol. 49, no. 7, pp. 1033 -1036.

[4] SCHEJBAL, V. Computing the electrical field strength of an antenna above an uneven earth. *Slaboproudy obzor* (in Czech), 1973, vol. 34, no. 12, pp. 541 - 547.

[5] KUPCAK, D. *ATC Radar Antennas. Environment Influence on ATC Radar Operation* (in Czech). Prague: MNO, 1986, vol. III.

[6] SCHEJBAL, V. Propagation over irregular terrain. *Radioengineering*, 1997, vol. 6, no. 1, pp. 19 - 22.

[7] SCHEJBAL, V. Comparison of propagation over irregular terrain. *Radioengineering*, 1997, vol. 6, no. 3, pp. 6 - 9.

[8] SCHEJBAL, V. Hybrid method for computation of propagation over irregular terrain. In *COST 280 Workshop*. Malvern (Great Britain), 2002, <http://www.cost280.rl.ac.uk>, CD-ROM.

[9] SCHEJBAL, V. et al. Czech radar technology. *IEEE Trans. Aerosp. Electron. Syst.* 1994, vol. 30, no. 1, pp. 2 - 17.

[10] UFIMTSEV, P. Ya. New insight into the classical Macdonald physical optics approximation. *IEEE Antennas Propag. Mag,* 2008, vol. 50, no. 3, pp. 11 - 20.

[11] SILVER, S. *Microwave Antenna Theory and Design.* New York: McGraw-Hill, 1949.

[12] Report 715-1. Propagation by diffraction. *Recommendations and reports of the CCIR*, 1982, vol. V, Propagation in non-ionized media, pp. 45 – 56.

[13] MEEKS, M. L. *Radar Propagation at Low Altitudes*. Dedham: Artech, 1982, Appendix C.

[14] PAPKELIS, E. G., et al. A Radio-coverage prediction model in wireless communication systems based on Physical Optics and the physical theory of diffraction. *IEEE Antennas Propag. Mag.,* 2007, vol. 49, no. 2, pp. 157 – 165.

[15] UFIMTSEV, P. Ya. Improved physical theory of diffraction: removal of the grazing singularity. *IEEE Trans. Antennas Propag.*, 2006, vol. 54, no. 10, pp. 2698 – 2702.

About Authors...

Vladimir SCHEJBAL graduated from the Czech Technical University, Prague in 1970. He received the PhD degree from the Slovak Academy of Science, Bratislava in 1980. He was with the Radio Research Inst. Opocinek, Czech Republic (Antenna Dept.) from 1969 to 1993. From 1983 to 1986, he was on a leave with the Higher Inst. of Electronics (Microwave Dept.) Beni Walid, Libya as a lecturer. He has been with the University of Pardubice, Czech Republic since 1994, now as a full professor and a head of the department. He is interested in microwave antennas and propagation. He has published over 140 papers. He is a senior IEEE member.

RADIOENGINEERING REVIEWERS

April 2009, Volume 18, Number 1